

SIMULATION OF H⁻ BEAM CHOPPING IN A SOLENOID-BASED LOW-ENERGY BEAM TRANSPORT (LEBT)*

Dan T. Abell[†], David L. Bruhwiler, Yongjun Choi, Sudhakar Mahalingam, Peter Stoltz,
Tech-X Corp., Boulder, CO, USA
Baoxi Han, Martin P. Stockli, Oak Ridge National Laboratory, Oak Ridge, TN, USA

Abstract

The H⁻ linac for the Spallation Neutron Source (SNS) includes an electrostatic low-energy beam transport (LEBT) subsystem. The ion source group at SNS is developing a solenoid-based LEBT, which will include MHz frequency chopping of the partly-neutralized, 65 keV, 60 mA H⁻ beam. Particle-in-cell (PIC) simulations using the parallel VORPAL framework are being used to explore the possibility of beam instabilities caused by the cloud of neutralizing ions generated from the background gas, or by other dynamical processes that could increase the emittance of the H⁻ beam before it enters the radio-frequency quadrupole (RFQ) accelerator.

INTRODUCTION

The Spallation Neutron Source (SNS) at Oak Ridge National Laboratory (ORNL) delivers nearly 1 MW of GeV protons to a spallation target, generating neutrons for materials science experiments. However, the present electrostatic low-energy beam transport (LEBT) system is vulnerable to losses from high power, high duty-factor beams and to sparks induced by high voltages in the source [1].

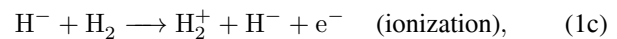
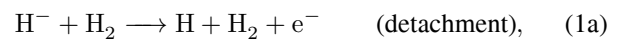
Solenoid-based LEBTs, on the other hand, do not spark, can withstand uncontrolled beam losses, and transport high-current, space-charge neutralized ion beams [2]. Hence, developing a magnetic LEBT with effective MHz frequency chopping of a 65 keV, 60 mA H⁻ beam is viewed as a critical reliability upgrade of the SNS for it to operate near and above 1 MW. Details can be found in [3].

The VORPAL plasma code [4, 5] includes a variety of physical models that make it useful for a broad range of research in plasma physics and computational electrodynamics. It can model a plasma as particles, a fluid, or a particle-fluid hybrid; it can treat electromagnetic fields either self-consistently or in the electrostatic limit; and it provides both explicit and implicit time updates.

PARTICLE COLLISIONS

In the SNS LEBT, energetic H⁻ ions collide with background residual H₂, creating positive ions and electrons, which interact further with the H⁻ beam and the background H₂. Because the results of these collisional processes can have a serious impact on the H⁻ beam trans-

port, we have added new capabilities to VORPAL so that it can now model a realistic chain of chemical reactions in a plasma. VORPAL's Monte Carlo collision (MCC) models, capable of handling electrons and positive ions colliding with background neutral particles, have now been extended to include electron detachment and ionization reactions between H⁻ ions and neutral H₂ and H gases. We can now track the following reactions:



The collision cross-sections needed for these reactions we implemented in T_XPHYSICS [6], a numerical library that includes atomic databases needed for modeling particle-particle and particle-surface interactions. The cross-sections for electron impact ionization of H₂ and H, Eqs. 1d and 1e, were already available in T_XPHYSICS. For the H⁻ electron detachment and H₂⁺ charge-exchange reactions, Eqs. 1a, 1b, and 1f, we have added cross-sections based on fitting functions and tabular data in [7, 8].

Of the reactions listed above, the largest cross-sections occur for H⁻ electron detachment, Eqs. 1a and 1b, at about 10⁻¹⁹ m² for 65 keV ions. The other reactions listed have cross-sections of order 10⁻²⁰ m² at the relevant electron and ion energies. Since it is the H₂⁺ and H⁺ species that neutralize our H⁻ beam, we conclude that realistic simulations should include the whole chain of chemical reactions.

VORPAL uses the statistical Monte Carlo collision (MCC) and null collision [9] algorithms to model the above reactions. In the null collision technique, one first determines the quantity ν_{max} , the maximum collision frequency possible in the plasma of interest. The probability P_{coll} of a collision event occurring during a given time step is based on ν_{max} and dt . And the the number N_{coll} of particles potentially involved in collisions is based on the product $N_{\text{macro}} \cdot P_{\text{coll}}$, where N_{macro} denotes the number of simulation particles. One randomly selects N_{coll} of the simulation particles, and then, for each one selected, determines the possible collision types and associated collision frequencies. A further random process, based on the ratio of collision frequency to ν_{max} selects the type of collision to apply. (This includes a possible null-collision, hence the name.)

*This work is supported by the US DOE Office of Science, Office of Basic Energy Sciences, including grant No. DE-SC0000844.

[†] dabell@txcorp.com

VORPAL then addresses the details of the chosen collision type.

To test the new VORPAL collision models, we applied them to a two-dimensional $0.4\text{ m} \times 0.4\text{ m}$ electrostatic (ES) simulation of a cold, 65 keV, 70 mA H^- beam of radius 13.5 mm. Our H^- beam traversed the domain from left to right. The top and bottom boundaries were held at 0 V (dirichlet boundary conditions), and they absorbed all particle species. On the left and right boundaries we enforced periodic boundary conditions for the electric field and for all particle species except the H^- beam, which we emitted from the left and absorbed on the right. In addition, we assumed a background H_2 gas pressure of 10^{-6} torr ($n_{\text{H}_2} = 3.22 \times 10^{16} \text{ m}^{-3}$). The simulation included all the reactions listed above in Eq. 1.

Using a computational grid of size 150×150 and a time step of 0.18 ns, we ran the simulation until the H^- beam became neutralized. Our initial results yield a neutralization time of about 250 μs . At least one source [10] states a neutralization time of about 50 μs —five times faster. Possible reasons for the discrepancy include (i) differences between the experimental and simulated plasmas, and (ii) chemical reactions not present in our simulation. We are continuing to investigate this issue.

VARYING THE MESH

In beam-plasma simulations, the beam may occupy a fraction of the entire simulated domain. In such cases, the use of a cell-size small enough to yield good resolution of the beam can lead to excessive computational demands. To address this issue, we have implemented a variable-mesh ES solver in VORPAL.

A VORPAL input file comprises a sequence of blocks that specify different aspects of a simulation. One of the required input blocks describes the computational grid. To describe a grid with a variable mesh, the new syntax makes possible the following example specification:

```
<Grid compGrid>
  kind = coordProdGrid
  coordinateSystem = Cartesian
  <CoordinateGrid dir0>
    sectionBreaks = [ X1  X2  X3  X4 ]
    deltaAtBreaks = [ DX1 DX2 DX3 DX4 ]
  </CoordinateGrid>
  <CoordinateGrid dir1>
    sectionBreaks = [ Y1  Y2  Y3 ]
    deltaAtBreaks = [ DY1 DY2 DY3 ]
  </CoordinateGrid>
  <CoordinateGrid dir2>
    sectionBreaks = [ Z1  Z2  Z3 ]
    deltaAtBreaks = [ DZ1 DZ2 DZ3 ]
  </CoordinateGrid>
</Grid>
```

In this example, the x -axis (dir0) is described between the pair of tags <CoordinateGrid dir0> and

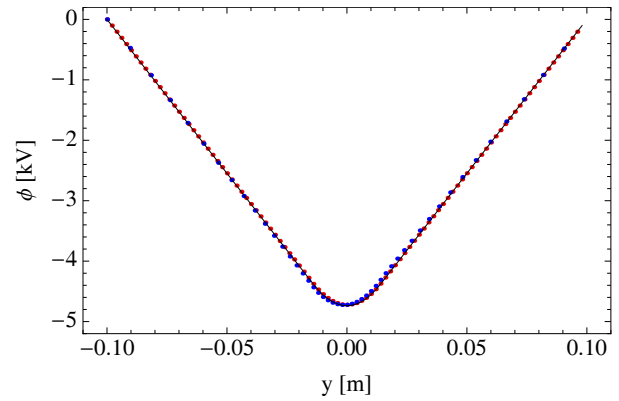


Figure 1: The potential computed for a simple test problem: uniform mesh (red), variable mesh (blue), analytic (black).

</CoordinateGrid>. Here we specify four locations, the *section breaks* X1, X2, X3, and X4, at which the mesh along the x -axis has the defined spacings DX1, DX2, DX3, and DX4. In response to this specification, VORPAL generates a varying mesh that matches our requirements; between adjacent section breaks, VORPAL's internal grid generator varies the grid spacing geometrically from one cell to the next.

For the variable-grid ES solver, VORPAL uses the following stencil for the Poisson equation:

$$\frac{\partial^2 \phi}{\partial x^2} = \frac{2}{x_{n+1} - x_{n-1}} \left(\frac{\phi_{n+1} - \phi_n}{x_{n+1} - x_n} - \frac{\phi_n - \phi_{n-1}}{x_n - x_{n-1}} \right). \quad (2)$$

Note that if $x_{n+1} - x_n = x_n - x_{n-1} = h_x$, then Eq. 2 reduces to the form

$$\frac{\partial^2 \phi}{\partial x^2} = \frac{\phi_{n-1} - 2\phi_n + \phi_{n+1}}{h_x^2}, \quad (3)$$

the standard stencil for a uniform-grid ES solver.

To test the variable-grid ES solver, we applied both it and a uniform-grid ES solver to a simple problem: a two-dimensional $0.2\text{ m} \times 0.2\text{ m}$ electrostatic (ES) simulation of an electron beam, radius 14.0 mm, traversing our domain from left to right. The top and bottom boundaries were held at 0 V (dirichlet boundary conditions), and on the left and right boundaries we enforced periodic boundary conditions. For the uniform grid, we used a computational domain of size 100×100 . And for the variable grid, we used a computational domain of size 100×48 . In the latter case, only the spacing transverse to the beam was varied. Across the beam itself, we used essentially the same cell-size as in the uniform case; then from the edge of the beam to the edge of the domain, we increased the transverse cell spacing until the last cells are five times wider than those in the center.

Figure 1 compares the results obtained by showing the computed potential along a line transverse to the beam. The red dots show the result produced by the uniform-grid ES solver. The blue dots, as their non-uniform spacing suggests, show that produced by the variable-grid ES solver. In the region near the beam, the maximum relative error is about 1.5%.

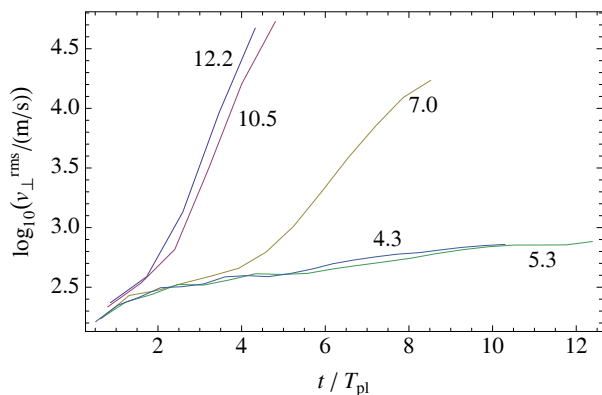


Figure 2: Growth of the rms velocity (in m s^{-1}) for several different beams. The time plotted on the horizontal axis is scaled to the plasma period, T_{pl} , of the corresponding beam. The annotations are current density in units of mA/cm^2

LEBT SIMULATION PLASMA DYNAMICS

Initial VORPAL simulations of the chopper covered the last 12.5 cm of the LEBT—after the solenoid and before the RFQ. These simulations did not exhibit instabilities. In order to understand the issues, we returned to some simpler scenarios. In one series of simulations, we modeled 66 cm of H^- beam traversing a neutralizing H_2^+ background. The current density differed in the different runs, but in all cases, (1) the H_2^+ ions initially fills the cylinder occupied by the initial H^- beam, (2) the H_2^+ is loaded at 300 K, (3) the 65 keV H^- beam is loaded cold, and (4) the H^- beam sees periodic boundary conditions in the longitudinal direction.

In the runs with the highest current densities, an instability readily shows up. As the current density drops, the instability becomes less severe. See Fig. 2, which shows the growth in the transverse rms velocity.

In a different set of simulations, we changed only the boundary conditions for the H^- beam—now emitting from one side and absorbing on the other. As Fig. 3 indicates, an instability does not appear until some 40 cm into the simulation. It appears that very long physical domains are necessary to ensure that we capture instabilities of interest. The beam shown in Fig. 3 corresponds to the 4.3 mA/cm^2 curve of Fig. 2, roughly the expected current density in the middle of the two-solenoid LEBT.

More recent simulations now model a slightly diverging H^- beam that is then focused by a solenoid down to a radius of about 1 cm. This corresponds to modeling the second half of the LEBT. In this case, to mimic the neutralization process, we loaded H_2^+ gradually. Despite using the same domain as shown in Fig. 3 and a 10% longer time, no instability appears. We are still investigating what suppresses the instability.

PUTTING IT ALL TOGETHER

We are now putting all the pieces together in our simulations. Figure 4 shows an image from a simulation that in-

Sources and Medium Energy Accelerators

Dynamics 05: Code Development and Simulation Techniques

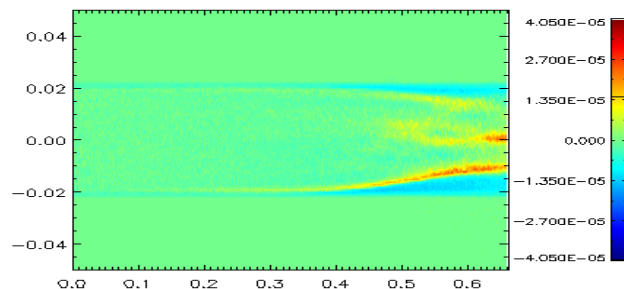


Figure 3: A 21 mm, 60 mA, H^- beam traverses a neutralizing H_2^+ background. This graphic shows the charge density in a vertical slice of the beam after 18 plasma periods.

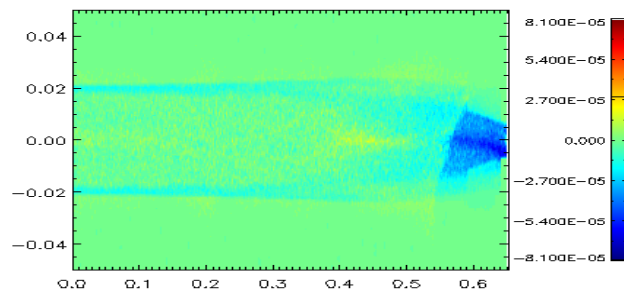


Figure 4: A 60 mA H^- beam with gradual neutralization, solenoid focusing, and chopper turned on. This graphic shows the charge density in a horizontal slice of the beam. Note the beam steering done by the chopper.

cludes both the second solenoid and the beam chopper turning on and off in a pattern that cyclically steers the beam left, up, right, and down. This simulation also includes some of the chemical reactions listed in Eq. 1.

In future work, we plan to include the full 2 m length of the two-solenoid LEBT in our simulations. These simulations will also include the full suite of chemical reactions expected to play a rôle in the LEBT plasma dynamics.

REFERENCES

- [1] B. Han and M.P. Stockli, PAC'2007, 1823–1825 (2007).
- [2] M.P. Stockli, LINAC'06, 213–217 (2006).
- [3] B. Han, D.J. Newland, W.T. Hunter, and M.P. Stockli, these proceedings.
- [4] C. Nieter and J.R. Cary, *J. Comput. Phys.*, 196:448 (2004).
- [5] P. Messmer and D.L. Bruhwiler, *Comput. Phys. Comm.*, 164:118 (2004). DOI: 10.1016/j.cpc.2004.06.018.
- [6] www.txcorp.com/products/TxPhysics/index.php
- [7] C.F. Barnett ed., ORNL-6086 V1, Oak Ridge (1990).
- [8] A.V. Phelps, *J. Phys. Chem. Ref. Data*, 19:653 (1990). DOI: 10.1063/1.555858.
- [9] V. Vahedi and M. Surendra, *Comput. Phys. Comm.*, 87:179 (1995). DOI: 10.1016/0010-4655(94)00171-W.
- [10] J.G. Alessi, J.M. Brennan, and A. Kponou, *Rev. Sci. Instrum.*, 61:625 (1990). DOI: 10.1063/1.1141939.